Available online at www.sciencedirect.com

ScienceDirect

IFAC Papers Online CONFERENCE PAPER ARCHIVE

IFAC-PapersOnLine 48-1 (2015) 737–742

Validation of a Simple Fouling Model for a Submerged Membrane Bioreactor

G. Araujo Pimentel [*,**] **M. Dalmau** [****] **A.Vargas** [***] **J. Comas** [****] **I. Rodriguez-Roda** [****,†] **A. Rapaport** [**] **A. Vande Wouwer** [*]

[*] *University of Mons, Automatic Control Laboratory, Bd. Dolez 31, 7000 Mons, Belgium* {*guilherme.araujopimentel;alain.vandewouwer*}*@umons.ac.be*

[**] *Equipe Projet INRIA MODEMIC, UMR MISTEA, Montpellier, France. rapaport@supagro.inra.fr*

[***] *Lab. for Research on Advanced Water Treatment Processes, Instituto de Ingeniería, Universidad Nacional Autónoma de México, Blvd. Juriquilla 3001, Juriquilla, Querétaro, 76230, México. avargasc@ii.unam.mx*

[****] *LEQUiA, Laboratory of Chemical and Environmental Engineering, University of Girona, Campus de Montilivi, E-17071 Girona, Catalonia, Spain* {*montse.dalmau; quim; ignasi*}*@lequia.udg.cat*

[†] *ICRA (Catalan Institute for Water Research), Scientific and Technological Park of the University of Girona, H2O Building c/Emili Grahit 101, E17003 Girona, Catalonia, Spain irodriguezroda@icra.cat*

Abstract: Most of the published membrane bioreactor (MBR) models have been proposed for process description and gain of insight, resulting in a large number of parameters to estimate from experimental data. These models are usually too complex for process control, and there is a need for simple, dedicated, dynamic models. In this study, attention is focused on the fouling phenomenon, which hampers the efficient operation of MBRs, and a simple model is proposed and validated using a large data base collected from a pilot plant. This model includes several manipulated variables, e.g., the permeate flow rate and the air scour, as well as a measurable perturbation such as the water temperature. To ease the identification procedure, a separation of the time scales of the process in slow and fast dynamics is exploited. The results show that the model can be used to predict the trans-membrane pressure behavior in a medium-term, about 10 days ahead.

Keywords: cake build-up; submerged membrane bioreactor; parameter estimation, model validation;

1. INTRODUCTION

The aerobic submerged membrane bioreactor (sMBR) has been increasingly applied to wastewater treatment (Judd and Judd, 2011), due to its high effluent quality (regarding solid matters), footprint reduction and the decoupling of the hydraulic and solid retention times. In its simple configuration, an sMBR combines the function of an activated sludge system with secondary and tertiary filtration in a single tank (Atasi et al., 2006). One of the main drawbacks of the sMBR process is the fouling phenomenon, caused by particles that attach to the membrane surface decreasing process efficiency and increasing energy consumption.

The dynamic behavior of such systems has been modeled with different degrees of detail (Ferrero et al., 2011; Li and Wang, 2006; Ferrero et al., 2012). The existing models range from the description of the physical interaction of constituents inside the cake on the membrane surface (Fenu et al., 2010; Naessens et al., 2012), to black-box mathematical models (Choi et al., 2012; Khan et al., 2009) that mimic the fouling build-up.

Most of these models are not appropriate for process control, as they are either too complex and contain parameters that are difficult to estimate from experimental data, or they lack physical interpretation. Simple dynamic models, in particular of the fouling mechanism, would however be very useful to optimize plant operation and develop controllers.

In the previous studies (Pimentel et al., 2015), a simple model combining biological and physical phenomena has been proposed and analyzed in terms of dynamics, time-scale separation, and equilibrium points. In the present contribution, attention is focused on the fouling mechanism only, and an even simpler dynamic model is proposed, calibrated and validated with experimental data collected from a pilot plant. With respect to the previous contributions, a new influence variable is also taken into account, namely the water temperature variation. To estimate the

2405-8963
Peer review under responsibility of International Federation of Automatic Control.
10.1016/j.ifacol.2015.05.031

model parameters, a time-scale separation approach is used, which allows subsets of parameters to be estimated independently. This study is organized as follows: Section 2 describes the sMBR process and its fouling model. Section 3 presents the fast and slow dynamics study. In Section 4 the pilot plant is presented, followed by model identification and validation with the experimental data in Section 5. Finally, in Section 6 some conclusions are drawn and perspectives are pointed out.

2. MODEL DESCRIPTION

Figure 1 shows a schematic representation of an sMBR process. The influent enters the reactor with a flow $Q_{in}[m^3/d]$ and concentrations $S_{in}[g/m^3]$ of substrate and $X_{in}[g/m^3]$ of solids. The permeate effluent is withdrawn with flow $Q_{out}[m^3/d]$, while $Q_w[m^3/d]$ is waste and recirculation flow. The input flow is equal to the sum of the permeate flow and the waste/recirculation flow. Usually, the latter is fixed to a constant value while the former is directly linked to the fouling resistance. The permeate flow rate Q_{out} and the bulk concentration $X[g/m^3]$ are responsible for the particle attachment onto the membrane surface, building-up the cake mass $m[g]$, which increases the trans-membrane pressure $TMP[mbar]$. To avoid this phenomenon sMBR are normally equipped with air diffusers at the bottom. The injected air flux $J_{air}[m^3/m^2d]$ produces the air scouring that aids in the detachment of the cake mass.

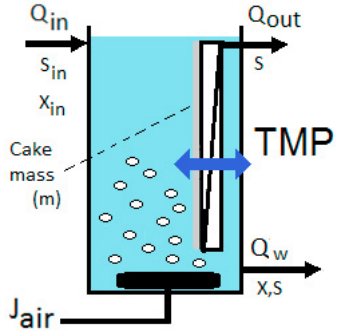

Fig. 1. Schematic representation of a submerged membrane bioreactor (sMBR).

In this study we consider a simple dynamic model, inspired by our previous work (Pimentel et al., 2015), to describe the fouling dynamics:

$$\begin{cases} \dfrac{d\beta}{dt} = \gamma\beta & \text{(1a)} \\ \dfrac{dm}{dt} = Q_{out}X - J_{air}\mu_{air}(m)m & \text{(1b)} \end{cases}$$

$$\mu_{air}(m) = \beta\frac{m}{K_{air}+m},$$

where the state vector includes the long-term cake evolution $\beta[m^{-1}]$ with $\beta(0) = \beta_0 > 0$ and the cake mass $m[g]$, with $m(0) = m_0 > 0$. Both states are positive and bounded if $\gamma < 0$; $\underline{Q_{out}} \leq Q_{out} \leq \overline{Q_{out}}$ is the permeate flow and $\underline{J_{air}} \leq J_{air} \leq \overline{J_{air}}$ is the air crossflow.

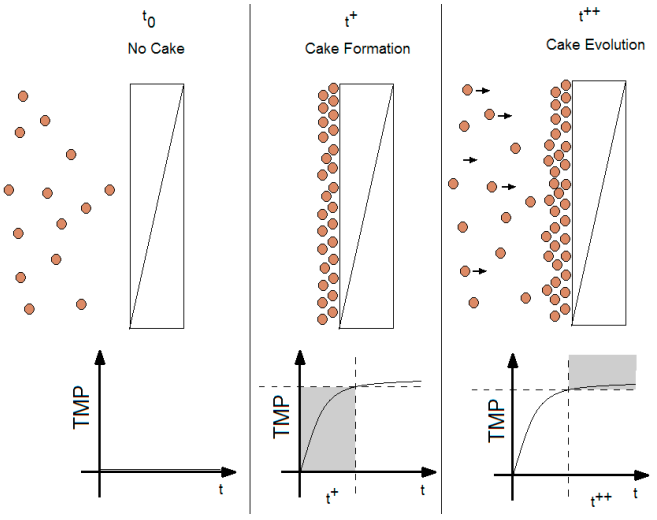

Fig. 2. t_0: Q_{out} is zero; t^+: the cake is formed; t^{++}: cake evolution

The long-term cake evolution β is a key factor of the model and represents the ease (or difficulty) of detaching the cake from the membrane by air scouring, influenced by the air crossflow J_{air}. Considering a process with constant permeate flow ($Q_{out} \approx constant$), the capacity of J_{air} to detach the cake decreases with time, due to the drag force on the solid particles, resulting in a decay behavior of β (difficulty of detachment), and thus $\gamma[d^{-1}]$ is a negative constant. Note that if the process has constant trans-membrane pressure ($TMP \approx constant$), the permeate flow decreases with time. Hence, β increases, and γ is positive, meaning that the efficiency of J_{air} increases as a consequence of the loss of the drag force of the membrane to the particle deposition. However, in this case the model should include a term limiting the growth of β to a practical maximum. Depending on the process setup (amplitude of permeate, waste and air flow, process relaxation and filtration cycles) the value of γ changes. Based on the observation of experimental data, one can conclude that this phenomenon has a slow behavior (Merlo et al., 2000), meaning that γ has a small value.

The nonlinear dynamic equation (1b) describes the cake dynamics evolution and its behavior is represented by Figure 2. The cake dynamic (dm/dt) is divided in two terms. The first term represents the attachment of suspended particles on the membrane surface, ruled by the permeate flow rate Q_{out} and suspended solids bulk concentration X. The second term represents the cake detachment proportional to air crossflow, that is governed by J_{air} and also by the cake mass m and $K_{air}[g]$, the half-saturation coefficient.

Usually, the cake mass cannot be measured due to the lack of reliable sensors (Dalmau et al., 2013). Thus, the trans-membrane pressure is used to indirectly control the cake build-up, according to the following equation (2):

$$TMP = \frac{Q_{out}}{A}\ \eta\ R_{total}. \qquad (2)$$

Q_{out} is the suction pump flow selected by the operator, $\eta[mbar \cdot d]$ is the apparent viscosity and $A[m^2]$ is the membrane area. The total fouling resistance, $R_{total}[m^{-1}]$, is modeled by

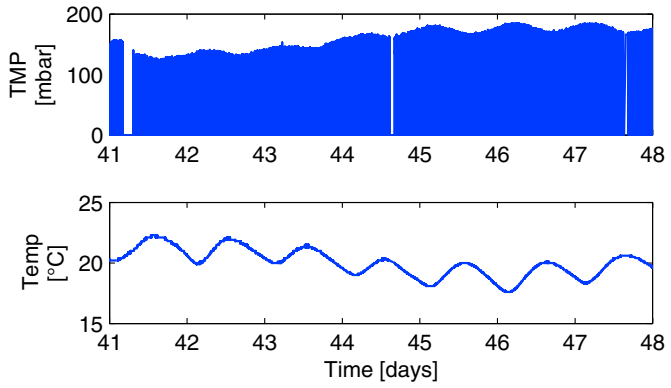

Fig. 3. The oscillations of the TMP and water temperature are approximately in phase opposition.

$$R_{total} = R_m + R_{cake} + \delta_R, \tag{3}$$

where $R_m[m^{-1}]$ is the intrinsic resistance (assumed constant) and δ_R is used to represent the total resistance disturbance, resulting from pore-blocking, biofilm, concentration polarization and scaling. R_{cake} is the cake resistance and, as previously reported (Lee et al., 2002; Khan et al., 2009), it is the most important term in the fouling build-up. Since R_m is proportionally small, the total resistance can thus be modeled as the cake resistance:

$$R_{cake} = \rho \frac{m + m_0}{A}, \tag{4}$$

where $\rho[m \cdot g^{-1}]$ is the specific cake resistance, $m_0[g]$ is the initial cake mass and $m[g]$ the cake mass.

It is important to remember that sMBR plants are exposed to daily temperature variations which have an influence on the temperature and the apparent viscosity of water. Figure 3 shows experimental data plots of water temperature and TMP. Note that the viscosity is inversely proportional to the water temperature. The apparent bulk viscosity η can be modeled by equation (5) proposed by Rodríguez et al. (2010):

$$\eta(Temp) = A_1 e^{\frac{A_2}{Temp}}, \tag{5}$$

where $Temp$ is the bulk temperature and A_1 and A_2 are apparent viscosity parameters.

3. FAST AND SLOW DYNAMICS ANALYSIS

Analyzing the model properties one can find that the process has at least two time-scales: long- and short-term. Thus, a singular perturbation analysis is applied to the model in order to reduce its apparent complexity. The method consists in finding a small positive parameter $(0 < \epsilon << 1)$ that will decouple the states according to fast and slow dynamics (Kokotović et al., 1986). Considering γ as a small parameter, and rewriting equation (1) with $\epsilon = \gamma$, $x = \beta$, $m = z$ and the stretched time-scale $\tau = \epsilon\, t$ we have:

$$\frac{dx}{d\tau} = x \qquad (Slow)$$
$$\epsilon \frac{dz}{d\tau} = Q_{out} X - x J_{air} \frac{z^2}{K_{air} + z} \qquad (Fast)$$

Since ϵ is small, on the slow time-scale the second dynamic equation degenerates into an algebraic equation and the fast part is considered in steady state (constant), while on the fast time-scale, the slow part variable (x) is assumed constant. This leads to a process separation into two time-scales: (1) cake build-up with complete detachment during the relaxation periods in the fast time-scale and (2) fouling evolution, slow time-scale. This means that the instantaneous attachment/detachment of the particles $(dm/dt$ dynamic) can be analyzed independently of the long-term evolution $(d\beta/dt)$. This decoupling will be exploited in the parameter identification procedure explained in Section 5.

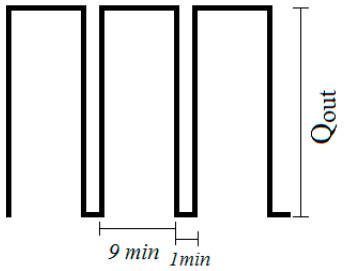

Fig. 5. Relaxation and permeate cycles, 1:9 minutes.

4. PILOT PLANT DESCRIPTION

The experimental pilot plant is an sMBR able to biologically remove organic matter, nitrogen and phosphorous, presented in Figure 4. The influent wastewater is obtained directly from the full-scale wastewater treatment plant sewer (at Castell d'Aro, Catalonia, Spain), where the MBR pilot plant is located. Specifically, the MBR pilot plant is equipped with a primary settler and a screening system to prevent the entrance of large particles. The bioreactor has a total volume of $2.26m^3$ divided in an anaerobic (14% of the total volume), an anoxic (14%) and an aerobic compartment (23%) and a compartment with submerged microfiltration flat sheet membranes (49%). The sludge retention time of the plant is $25 \pm 6d$, and the hydraulic retention time is $0.50 \pm 0.05d$. The total area of the membrane used is $8m^2$ (LF, Kubota, Japan), with a nominal pore size of $0.4\mu m$, working at 9 minutes filtration and 1 minute relaxation; see Figure 5. The permeate production is around $3.6m^3/d$, and membrane aeration fluctuates between $27 - 36m^3/m^2d$, depending on the fouling behavior. The suspended solids concentration in the membrane compartment ranges from $6-10g/l$, while in the anaerobic reactor, it varies between $1-3g/l$. On-line data, including temperature, flows, suspended solids concentration (into the membrane and in the anaerobic tank), air-flow rates and dissolved oxygen concentration, are gathered every 10 seconds.

5. MODEL IDENTIFICATION AND VALIDATION

The objective of identification is to infer a set of parameters from experimental data such that the proposed dynamic model can mimic the sMBR process behavior with a satisfactory accuracy. The procedure is based on the minimization of a cost function measuring the deviation between experimental data and model outputs.

In order to fit the response of the fouling model to the experimental data collected from plant, the unweighted least-squares cost function

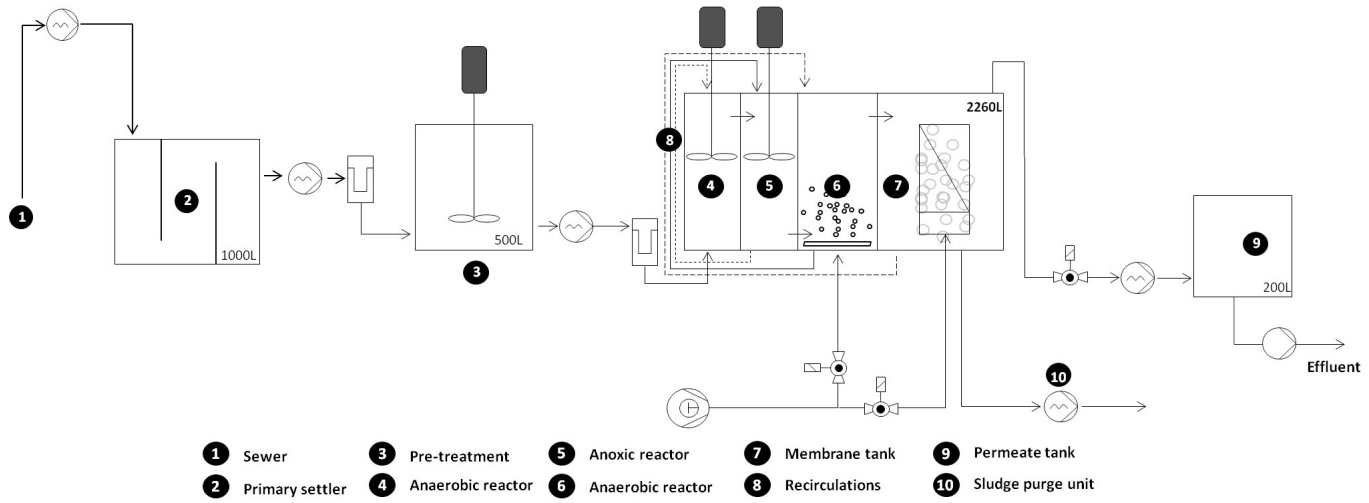

Fig. 4. Experimental pilot plant schematic.

$$J(\theta) = \sum_{i=1}^{n_t} \left((\xi_{sim}(i)\xi_{pilot}(i))\right)^T \left((\xi_{sim}(i) - \xi_{pilot}(i))\right) \quad (6)$$

is minimized, where $\xi_{pilot} = [TMP]$, $\xi_{sim} = [TMP_{sim}]$, $\theta = [K_{air}, \rho, m_0, \gamma, A_1, A_2]$ and n_t is the number of measurements. The optimization is performed in this study using the Nelder-Mead algorithm as implemented by the *fminsearch* function in *Matlab*. This method is selected due to its simple implementation, a rapid asymptotic convergence is not priory important and the experimental data set could have missing, noisy and non-smooth measurements, which could be a problem if a gradient method is implemented.

A lower bound on the covariance matrix $\hat{P}$ of the parameter estimates is obtained by the inverse of the Fisher Information Matrix (FIM):

$$\hat{P} = F^{-1}(\hat{\theta}, \Omega) \quad (7)$$

The FIM is computed by:

$$F(\hat{\theta}) = \sum_{i=1}^{n_t} \left[\frac{\partial Y_m}{\partial \theta}\right]^T_{(t_i,\hat{\theta})} \Omega^{-1} \left[\frac{\partial Y_m}{\partial \theta}\right] \quad (8)$$

where Y_m is the vector of the process outputs, Ω is the estimate covariance matrix

$$\Omega = \frac{J(\hat{\theta})}{(n_t - p)} I \quad (9)$$

and p is the number of parameters to be estimated.

The square root σ_j of the j^{th} diagonal element of $\hat{P}$ is an estimate of the standard deviation of $\hat{\theta}$, which is used to obtain the parameters confidence intervals of 2.56σ corresponding to a probability of 99%.

The initial parameter values have been inspired by physical interpretation, literature study and knowledge about process dynamic behavior. The parameters ρ and m_0 influence the TMP initial amplitude and K_{air} the detachment by J_{air}; γ is linked to the TMP slope and A_1 and A_2 define the apparent viscosity. Before starting the validation procedure, the three month data set is analyzed and a data window is selected based on the following properties:

(1) It should contain data for the model input and output comparison, i.e. Q_{out}, J_{air}, X and $Temp$ for model inputs and TMP for model output. These measurements are essential for the process simulation;
(2) Data with TMP lower then 20 $mbar$ are not considered;
(3) No or small data acquisition interruption.

Based on the fast and slow dynamics analysis presented on Section 3, the parameter identification can be organized in two steps corresponding to the two time-scales. The set of parameters θ is divided in two subsets of parameters to be identified. Indeed, a direct identification of all the parameters at once is delicate and leads to the occurrence of several local minima. A divide and conquer approach is therefore used, where one subset of parameters is estimated first, and the second subset of parameters is then estimated starting from the previous estimates (which are then much closer to the optimum and severely decrease the computation efforts). The short-term identification procedure uses $\theta_{short} = [K_{air}, \rho, m_0]$ with β and η considered constant values. Note that the viscosity(η) can be measured and β should be roughly estimated by some preliminary simulations. The identified short-term parameters are used in the long-term identification, that has a long-term parameters subset $\theta_{long} = [\gamma, A_1, A_2]$.

5.1 Short-term identification and validation

As presented in Figure 6, the fast behavior of cake attachment and detachment, which influence the TMP measurements, is evident. With that, the short-term parameters are estimated and validated analyzing only the fast dynamics of the process (dm/dt). The parameters identification procedure is set to have a half day of data simulation to identify K_{air}, ρ and m_0, from days 20.0 to 20.5. Table 1 shows the identified parameters values found by minimization of the cost function (6).

Figure 7 shows the simulation results that have a correlation factor of $R^2 = 0.9518$. Following the procedure, the short-term identified parameters are used for the identification of the long-term parameters. Note that the slow phenomena do not interfere in the fast dynamics, meaning

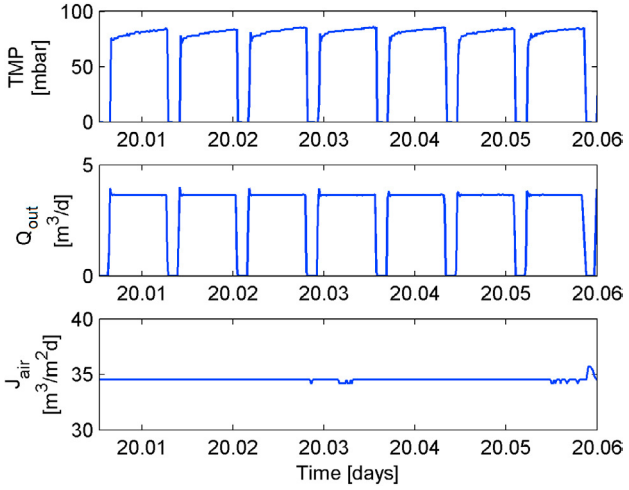

Fig. 6. TMP short-term behavior.

Table 1. Short-term: Identified parameters

Short-term Parameters	Values
K_{air} $[g]$	19.2725 ± 0.0001
ρ $[m/g]$	$33.9329 \times 10^{13} \pm 1.459 \times 10^{-2}$
m_0 $[g]$	$1288 \pm 3.9646 \times 10^{-2}$
β $[m^{-1}]$	30 (Constant Value)
η $[mbar \cdot d]$	2.66 (Constant Value)

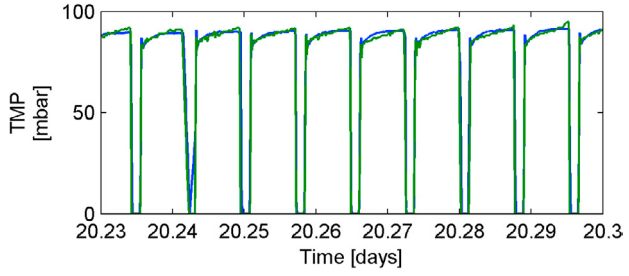

Fig. 7. Short-term validation: blue is the model and green is the experimental data.

that the slow phenomena do not exist in a short period of time, i.e. 0.5 days.

5.2 Long-term identification and validation

For the long-term validation the larger data set is used, i.e. from days 20 to 50. The parameters γ, A_1 and A_2 are thus identified. Their estimated values and sensitivities are shown in Table 2.

Table 2. Long-term: Identified parameters

Long-term Parameters	Values
K_{air} $[g]$	Short-term identified (see Tab.1)
ρ $[m/g]$	Short-term identified (see Tab.1)
m_0 $[g]$	Short-term identified (see Tab.1)
γ $[1/d]$	-0.0641 ± 0.0050
A_1	1.3304 ± 0.0011
A_2	13.648 ± 0.0055

Figure 8 shows experimental data TMP, Q_{out}, J_{air}, $Temp$ and X in blue lines. In green is the model simulation. The correlation factor of TMP is $R^2 = 0.9630$. Note that the model follows the day water temperature oscillations. It is important to highlight that if these oscillations are not

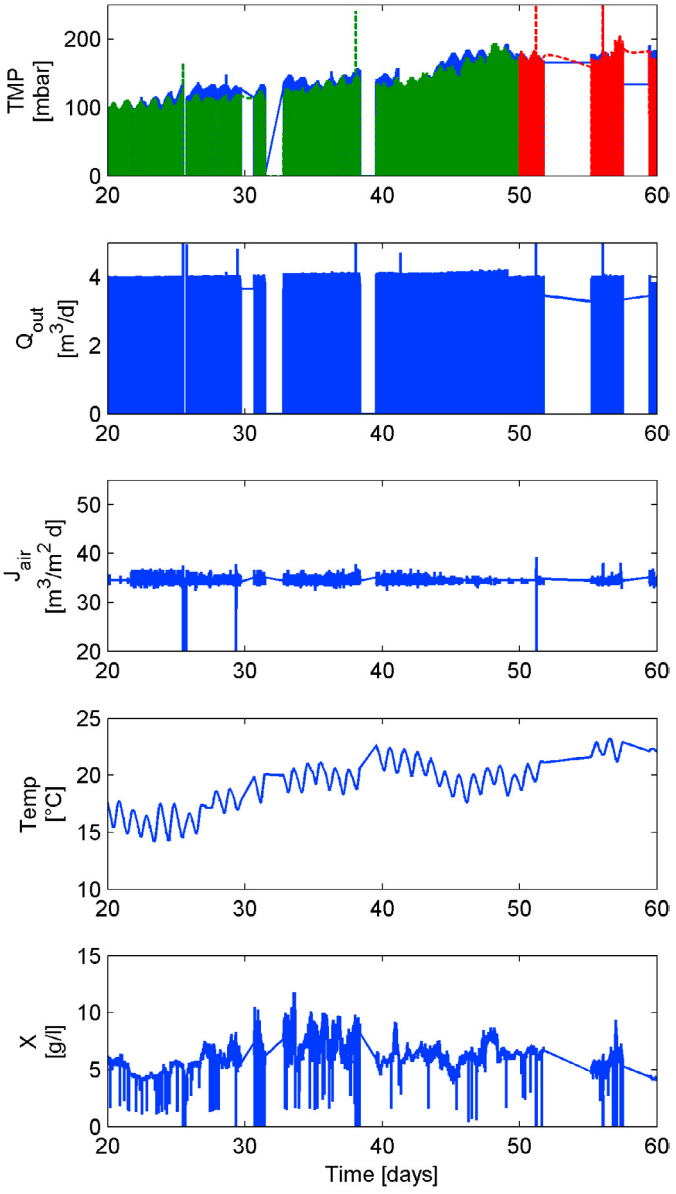

Fig. 8. Long-term validation: blue line is the experimental data, green line is the identified model and red line is the predicted values

considered and the process is not analyzed in a long-term, a wrong interpretation of the TMP measurement could be mistakenly made: one may think that the TMP is decaying, but this is only due to the temperature affecting the bulk apparent viscosity, and not to some implemented control scheme. Taking account of these natural variations may indeed lead to better fouling control strategies.

5.3 Cross-validation

The cross-validation analysis is done with a set of data that have not been used for identification purposes. In this study the cross-validation period is done from days 50 to 60. This simulation is presented in Figure 8 by the red line, and in more details in Figures 9 and 10. Even though these 10 days of data were not used for the identification routine, they still have a TMP correlation factor of $R^2 = 0.9512$, showing the capacity of the model

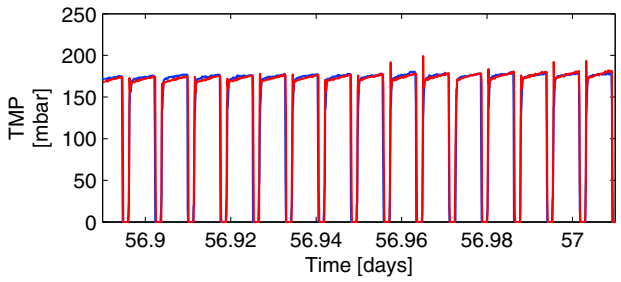

Fig. 9. Short-term cross-validation. Blue line is the experimental data and red line is the predicted values

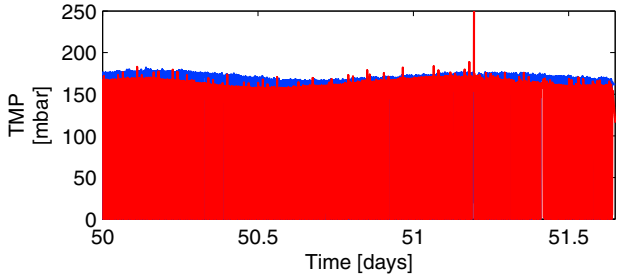

Fig. 10. Long-term cross-validation detail. Blue line is the experimental data red line is the predicted values

to predict TMP in a medium-term horizon. Note that this simple model captures the main dynamics of the process, with few parameters. If more accuracy is needed, more complex dynamics could be modeled and added to the model. It is important to emphasize that although there are small missing data periods, the model continues to predict the process quite well.

6. CONCLUSION

The proposed model for an sMBR process has been validated with a large quantity of experimental data, in short and long terms. The TMP dynamics can be reproduced by the model with an accuracy around $R^2 = 0.95$ validating the model horizon prediction propriety. The time-scale separation based on the fast and slow study simplified and decreased the computational effort on the parameter identification procedure, resulting in the possibility for on-line prediction of TMP. As future work, the capacity of the model to predict TMP evolution in real-time and TMP model-based process control will be studied.

ACKNOWLEDGEMENTS

This paper presents research results of the Belgian Network DYSCO (Dynamical Systems, Control, and Optimization), funded by the Interuniversity Attraction Poles Programme, initiated by the Belgian State, Science Policy Office. Alejandro Vargas has been beneficiary of a post-doc grant from Belgium Science Policy Office (BELSPO). The scientific responsibility lies with its authors.

REFERENCES

Atasi, K., Crawford, G., Hudkins, J.M., Livingston, D., Reardon, R., and Schmidt, H. (2006). *Membrane systems for wastewater treatment*. WEFPress.

Choi, Y.J., Oh, H., Lee, S., Nam, S.H., and Hwang, T.M. (2012). Investigation of the filtration characteristics of pilot-scale hollow fiber submerged MF system using cake formation model and artificial neural networks model. *Desalination*, 297, 20–29.

Dalmau, M., Rodríguez-Roda, I., Ayesa, E., Odriozola, J., Sancho, L., and Comas, J. (2013). Development of a decision tree for the integrated operation of nutrient removal MBRs based on simulation studies and expert knowledge. *Chemical Engineering Journal*, 217, 174 – 184.

Fenu, A., Guglielmi, G., Jimenez, J., Sprandio, M., Saroj, D., Lesjean, B., Brepols, C., Thoeye, C., and Nopens, I. (2010). Activated sludge model (asm) based modelling of membrane bioreactor (mbr) processes: A critical review with special regard to mbr specificities. *Water Research*, 44, 4272 – 4294.

Ferrero, G., Rodriguez-Roda, I., and Comas, J. (2012). Automatic control systems for submerged membrane bioreactors: a state-of-the-art review. *Water Research*, 46 (11), 34213433.

Ferrero, G., Moncús, H., Buttuglieri, G., Gabarron, S., Comas, J., and Rodríguez-Roda, I. (2011). Development of a control algorithm for air-scour reduction in membrane bioreactors for wastewater treatment. *Journal of Chemical Technology and Biotechnology*, 86 (6), 784 – 789.

Judd, S. and Judd, C. (2011). *The MBR book, principles and applications of membrane bioreactors in water and wastwater treatment*. Elsevier, second edition.

Khan, S.J., Visvanathan, C., and Jegatheesan, V. (2009). Prediction of membrane fouling in mbr systems using empirically estimated specific cake resistance. *Bioresource Technology*, 100(23), 6133 – 6136.

Kokotović, P., Khalil, H.K., and O'Reilly, J. (1986). *Singular Pertubation Methods in Control:Analysis and Design*. Academic Press INC.(London)LTD.

Lee, Y., Cho, J., Seo, Y., Lee, J.W., and Ahn, K.H. (2002). Modeling of submerged membrane bioreactor process for wastewater treatment. *Desalination*, 146, 451 – 457.

Li, X.y. and Wang, X.m. (2006). Modelling of membrane fouling in a submerged membrane bioreactor. *Journal of Membrane Science*, 278(1-2), 151 – 161.

Merlo, R.P., Adham, S., Gagliardo, P., Trussell, R.S., Trussell, R., and Watson, M. (eds.) (2000). *Application of membrane bioreactor (MBR) technology for water reclamation*, volume 27. Proceedings of the Water Environment Federation, WEFTEC 2000: Session 11 through Session 20, Water Environment Federation.

Naessens, W., Maere, T., and Nopens, I. (2012). Critical review of membrane bioreactor models - part 1: Biokinetic and filtration models. *Bioresource Technology*, 122, 95 – 106.

Pimentel, G.A., Vande Wouwer, A., Harmand, J., and Rapaport, A. (2015). Design, analysis and validation of a simple dynamic model of a submerged membrane bioreactor. *Water Research*, 70, 97–108.

Rodríguez, F..A., M.V., M.T., González-López, J., Hontoria, E., and Poyatos, J. (2010). Performance of benchscale membrane bioreactor under real work conditions using pure oxygen: Viscosity and oxygen transfer analysis. *Bioprocess and Biosystems Engineering*, 33, 885 – 892.